반 최적화기법에 의한 적층복합보의 손상추적

Damage Detection in Laminated Beams by Anti-Optimization

이 재 홍*
Lee, Jae-Hong

요 약

본 연구는 적층복합보에 있어서의 층간분리현상을 추적하는 기법을 소개하고 있다. 이 기법에서는 층간분리된 보와 층간분리되지 않은 보와의 응답차이를 최대화하도록 조화운동의 가력을 보위별로 최적화한다. 2개층의 알루미늄 보에 대하여 수치해석을 수행하였으며, 계측 및 보의 형태에 따른 노이즈를 고려하였다. 층간분리를 모델링하기 위하여 스텝함수를 사용하였으며 층별복합판 이론에 기본한 유한요소법을 이용하여 해석하였다.

Abstract

The present study proposes a detection technique for delaminations in a laminated compoiste structure. the proposed technique optimizes the spatial distribution of harmonic excitation so as to magnify the difference in response between the delaminated and intact structures. The technique is evaluated by numerical simulation of two-layered aluminum beams. Effects of measurement and geometric noises are included in the analysis. A finite element model for a delaminated beam, based on the layer-wise laminated plate theory in conjunction with a step function to simulate delaminations, is used.

Keywords : delamination, anti-optimization

1. INTRODUCTION

Delamination is one of the most commonly observed damage modes in laminated composites. It may develop as a result of manufacturing defects or in-service events such as low velocity impact. Delaminations are not readily identified by visual inspection since they are cracks in the interior of the laminate.

Delaminations are known to cause a change in vibration frequencies and mode shapes of laminated composites. The delaminated sublaminate generally exhibits new vibration modes and frequencies that depend on the size and location of the delamination. Thus, provided that the natural frequencies and mode shapes

* 정회원 · 현대건설 기술연구소 선임연구원

• 이 논문에 대한 토론을 1996년 12월 31일까지 본 학회에 보내주시면 1997년 6월호에 그 결과를 게재하겠습니다.

are known for a composite containing delaminations, the presence of invisible delaminations can be detected, and their size and location can further be estimated.

Not much research has been done on detecting the existence and location of delaminations in laminated composites. Hanagud et al.[1] proposed a method to detect a delamination in a laminated beam by comparing the vibration signature of a delaminated beam with an intact beam. They showed that it is difficult to assess the size and location of the delamination from the time response itself, and that care must be taken to calibrate the sensor response to detect the delaminations. Teboub and Hajela[2] proposed a neural network based strategy for detecting delamination, fiber breakage, and matrix cracking in laminated composites. They computed the slopes of the strains at the measurement points by using piezoelectric sensors. Kim, et al.[3] used strain sensors on the surface and inside the material for detecting delaminations in laminated composites. Their results suggested that numerous sensors would be needed for large structures.

In the present paper, a finite element model based on the layer-wise laminated plate theory[4] is used to compute the steady state response of delaminated and intact beams. Then, an anti-optimization strategy is used in conjunction with system identification techniques for detecting a delamination. Anti-optimization is a method for maximizing differences between alternative models. Haftka an Kao[5] maximized the ratio and difference between two laminated composite failure models by varying the loading, the geometry, and lamination angles. Gangadharan et al.[6] sought the loads that maximize the difference in strain energies between two finite element models. They showed that the optimal discriminating loading was the solution to a generalized eigenvalue problem.

In this paper, ratios of strain energies are considered as a measure of the difference between intact and delaminated beams. The ratios are then maximized by solving eigenvalue problems. After obtaining the excitation which maximizes the response ratio between delaminated and undelaminated beams, this excitation is used to detect the location of delamination as a force input in a residual force calculation.

2. DYNAMIC MODELLING OF DELAMINATION

The notation here follows that of Lee et al.[4] To model multiple delaminations, the displacement field is supplemented with unit step functions which allow discontinuities in the displacement field (Fig. 1). The resulting displacements u_1 and u_3 at a generic point x, z in the laminate and time t are assumed to be of the form:

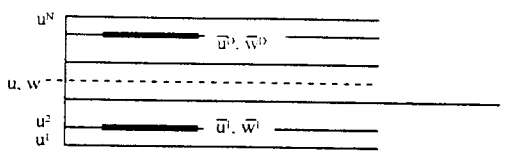

Fig. 1 Kinematics of layerwise theory with delaminations

$$u_1(x,z,t)=u(x,t)+\phi^j(z)u^j(x,t)+\delta^i(z)\bar{u}^i(x,t),$$
$$u_3(x,z,t)=w(x,t)+\delta^i(z)\bar{w}^i(x,t). \quad (1)$$

The superscripts i and j range from 1 to D and 1 to M, respectively, where D is the number of delaminations, and M is the number of layers of a composite. Repeated indices are tensor notation.

The terms u and w are the displacements of a point(x,0,t) on the reference surface of the laminate, u^j are nodal values of the displace-

ments in the x direction of each layer, and $\bar{u}^i$ and $\bar{w}^i$ represent possible jumps in the slipping and opening displacements respectively at the L(i)th delaminated interface. L(i) denotes the location of the interface where the i^{th} delamination lies. $\phi^j(z)$ and $\delta^i(z)$ denote a linear interpolation function through the thickness of the laminate and unit step function, respectively.

The Euler-Lagrange equations of motion of the presente theory can be derived from the Hamilton's principle:

$$N_{x,x} = I^0\ddot{u} + I^j\ddot{u}^j + \bar{I}^i\ddot{\bar{u}}^i, \tag{2a}$$

$$Q_{xz,x} = I^0\ddot{w} + \bar{I}^i\ddot{\bar{w}}^i, \tag{2b}$$

$$N^j_{x,x} - Q^j_{xz} = I^j\ddot{u} + I^{jk}\ddot{u}^k + \bar{I}^{ij}\ddot{\bar{u}}^i, \tag{2c}$$

$$\bar{N}^i_{x,x} = \bar{I}^i\ddot{u} + \bar{I}^{ij}\ddot{u}^j + \bar{I}^{ir}\ddot{u}^r, \tag{2d}$$

$$\bar{Q}^i_{xz,x} = \bar{I}^i\ddot{w} + \bar{I}^{ir}\ddot{w}^r, \tag{2e}$$

where i,r=1,⋯,D and j,k=1,⋯,M. The stress resultants are

$$[N_x, N^j_x, \bar{N}^i_x] = \int_{-h/2}^{h/2} \sigma_x[1, \phi^j, \delta^i]dz,$$

$$[Q_{xz}, Q^j_{xz}, \bar{Q}^i_{x,z}] = \int_{-h/2}^{h/2} \tau_{xz}[1, \phi^j_{,z}, \delta^i]dz, \tag{3}$$

and the inertia coefficients are defined as

$$[I^0, I^j, \bar{I}^i] = \int_{-h/2}^{h/2} \rho_x[1, \phi^j, \delta^i]dz,$$

$$[I^{jk}, \bar{I}^{ij}, \bar{I}^{is}] = \int_{-h/2}^{h/2} \rho_x[\phi^j\phi^k, \delta^i\phi^j, \delta^i\delta^s]dz, \tag{4}$$

where ρ is the material density. A more detailed mathematical formulation can be found in Lee et al.[4]

To obtain finite element equations, the generalized displacements (u, w, u^j, $\bar{u}^i$, $\bar{w}^j$) are expressed over each element as a linear combination of the one-dimensional interpolation functions ψ_l and the nodal values:

$$(u, w, u^j, \bar{u}^i, \bar{w}^j) = \sum_{l=1}^{n} (u, w, u^j, \bar{u}^i, \bar{w}^j)_l \psi_l. \tag{5}$$

Substituting these expressions into the weak statement, the finite element model of a typical element can be obtained. By assemblying the element matrices, the global stiffness and mass matrices (K and M) can be obtained.

3. ANTI-OPTIMIZATION

The anti-optimization technique seeks conditions that maximize the difference between two models. Here anti-optimization is used to obtain the frequency and spatial distribution of excitations that maximize the difference between the delaminated and intact beams under harmonic excitation. First, consider the equation of motion of a delaminated beam under harmonic excitation delivered by N actuators

$$M\ddot{U} + KU = H\, f e^{iwt}, \tag{6}$$

where ω denotes the exitation frequency, M and K are n×n mass and stiffness matrices, respectively, of a delaminated beam with n being the number of total degrees of freedom of the beam. H is a real matrix which indicates the locations of actuators, and f is an actuator input vector with dimension N.

Since the excitation is harmonic, so is the response

$$U = u\, e^{iwt}, \tag{7}$$

Thus, Eq. (6) becomes

$$(K - \omega^2 M)u = Hf. \tag{8}$$

To use anti-optimization, a measure of the difference in the response between the damaged and intact beams is needed. In this work,

strain energy measure is considered as described below.

Excitations which maximize the ratio E_1 of strain energies between delaminated and nominal structures was sought.

$$E_1 = \frac{u^T K u}{u_o^T K_o u_o} \tag{9}$$

where u and u_o are the displacement vectors of delaminated and intact beams for a given excitation, respectively. K_o is the stiffness matrix of an intact beam. Anti-optimization looks for the excitation that maximizes E_1.

At the same time, the calculated displacement fields u should not be associated with very high natural frequencies, because suh fields typically have small amplitudes and are difficult to measure. This imposes the constraint.

$$E_2 = \frac{u^T K u}{u^T M u} < \omega_o^2 \tag{10}$$

where ω_o is a limit frequency.

These two requirements can be combined by minimizing

$$\frac{1}{E_1} - \lambda \frac{1}{E_2}, \tag{11a}$$

or, alternatively, maximizing

$$E_3 = \frac{u^T K u}{u_o^T K_o u_o - \lambda u^T M u}, \tag{11b}$$

where λ is a positive weighting factor. Since the frequency and spatial distribution of excitation is to be selected, Eq. (11b) is transformed in terms of excitation.

From Eq.(8), u can be obtained as

$$u = (K - \omega^2 M)^{-1} H f. \tag{12}$$

Similarly for the undelaminated beam,

$$u_o = (K_o - \omega^2 M_o)^{-1} H f. \tag{13}$$

Now Eq. (11b) can be rewritten as

$$E_3 = \frac{f^T \hat{K} f}{f^T \hat{D} f}, \tag{14a}$$

where

$$\begin{aligned} \hat{K} &= H^T (K - \omega^2 M)^{-1} K (K - \omega^2 M)^{-1} H, \\ \hat{D} &= \hat{K}_o - \lambda \hat{M} \\ \hat{K}_o &= H^T (K_o - \omega^2 M_o)^{-1} K_o (K_o - \omega^2 M_o)^{-1} H, \\ \hat{M} &= H^T (K - \omega^2 M)^{-1} M (K - \omega^2 M)^{-1} H \end{aligned} \tag{14b}$$

are generalized flexibility matrices associated with the two models. Eq. (14a) indicates that E_3 is a Rayleigh quotient, so that its extreme values are the extreme eigenvalues of the generalized eigenvalue problem:

$$(\hat{K} - E_3 \hat{D}) f = 0. \tag{15}$$

For a given set of actuator locations and excitation frequency, the actuator excitation amplitude vector that extremizes E_3 is the eigenvector of the eigenproblem of Eq. (15).

Stiffness and mass matrices of the delaminated beam (K and M) are unknown in general, but $\hat{K}$ and $\hat{M}$ can be determined experimentally by measuring the displacements at the actuator locations. The functional E_3 in Eq.(11b) can be rewritten using Eq.(8) as:

$$E_3 = \frac{u^T H f + \omega^2 u^T M u}{u_o^T K_o u_o - \lambda u^T M u} = \frac{\hat{u}^T f + \omega^2 u^T M u}{u_o^T K_o u_o - \lambda u^T M u}, \tag{16}$$

where $\hat{u} = H^T u$ is a reduced displacement vector corresponding to the locations of actuators. Displacements at each actuator location of the beam need to be measured under the action of a unit load applied at each actuator, one at a

time. The total displacement at each actutor location is then obtained as

$$\hat{u}_i = S_{ij} f_j, \tag{17}$$

where S_{ij} is the displacement generated at the ith actuator location due to a unit load applied to the jth actuator. The flexibility matrix H can be expressed with the aid of Eq. (12) as:

$$S = H^T(K - \omega^2 M)^{-1} H. \tag{18}$$

The quantity $u^T Mu$ can be determined from the derivative of H with respect to ω^2. That is,

$$\frac{\partial S}{\partial(\omega^2)} = H^T(K-\omega^2 M)^{-1} M (K-\omega^2 M)^{-1} H = \hat{M} \tag{19}$$

Therefore, it can be written

$$u^T Mu = f^T \frac{\partial S}{\partial(\omega^2)} f. \tag{20}$$

Note that the quantity $\partial S/\partial(\omega^2)$ can be experimentally estimated by measuring H for several different frequencies ω. Finally, the functional $E_3 = f^T \hat{K} f / f^T \hat{D} f$ from Eq. (14a) is now expressed as:

$$\hat{K} = S + \omega^2 \frac{\partial S}{\partial(\omega^2)},$$
$$\hat{D} = \hat{K}_o - \lambda \frac{\partial S}{\partial(\omega^2)}. \tag{21}$$

where H is measured for the damaged structure, and $\hat{K}_o$ is calculated analytically from a model of the intact structure. If a good model of the intact structure is unavailable, $\hat{K}_o$ can be also neasured as:

$$\hat{K}_o = S_o + \omega^2 \frac{\partial S_o}{\partial(\omega^2)}, \tag{22}$$

where

$$S_o = H^T(K_o - \omega^2 M_o)^{-1} H. \tag{23}$$

4. SYSTEM IDENTIFICATION

After anti-optimization is performed successfully, identifying the location of delamination in the sturcutre is based on the differences in responses of delaminated and intact structures in conjunction with anti-optimization. Assume that the stiffness and mass in matrices of a del- and Garba[7], can be defined as

$$K = K_o + \eta_i \Delta K_i,$$
$$M = M_o + \eta_i \Delta M_i, \tag{24}$$

where η_i is an amplitude coefficient and ΔK_i and ΔM_i are differences in stiffness and mass matrices for the ith delamination location, respectively. The subscript i indexes the simulated delaminations.

Using Eq. (24) and Eq. (13), residual force vector R, which is similar to the one in Chen and Garba[7], can be defined as

$$(K-\omega^2 M)u_o - Hf = \eta_i(\Delta K - \omega^2 \Delta M)_i u_o \equiv R. \tag{25}$$

The partial derivative of the residual force R with respect to the parameter η_i becomes

$$\frac{\partial R}{\partial \eta_i} = (\Delta K - \omega^2 \Delta M)_i u_o. \tag{26}$$

Observe that $(\Delta K - \omega^2 \Delta M)_i$ can be predetermined for all simulated delamination locations. The displacement vector of an intact structure u_o in Eq. (26) is calculated from Eq. (13) with an anti-optimization solution as a force vector f. The partial derivatives of the residual force are calculated for all degrees of freedom of the

beam, and later they are lumped into a parameter for each finite element node.

The delamination location is assumed to be the region where the derivative of residual force is high. When there is more than one peak in the residual force response, all the candidate locations are investigated further as follows: Find the maximum excitation ratio and corresponding eigenvector f^c for a given external frequency ω using the anti-optimization method described in the previous section for all candidates. Then the angles between the solution f of the original (measured) system with unknown delamination and the candidates f^c are calculated as:

$$\theta = \arccos\left(\frac{|f \cdot f^c|}{||f||\ ||f^c||}\right),\ 0° \le \theta \le 90°. \quad (27)$$

The candidate whose eigenvector makes the smallest angle with the measured eigenvector is considered to be the actural location of delamination. After determining the delamination location, the delamination size can be estimated by comparing the eigenvalue of candidate size with experimentally achieved eigenvalue.

5. NUMERICAL EXAMPLES

A simply-supported aluminum beam of length l=3ft and thickness h=0.5in with a delamination at the midplane is considered for numerical investigation(Fig. 2); material properties are

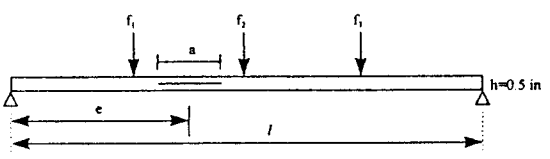

Fig. 2 A simply-supported beam with a delamination with midplane

$$E=10^7 \text{ psi},\ \nu=0.3$$

$$\rho=0.1\frac{\text{lbm}}{\text{in}^3}=0.259\times10^{-3}\frac{\text{lb}\cdot\text{s}^3}{\text{in}^4}. \quad (28)$$

A 7.2in delamination (20% of the beam span) is assumed to be centered at the location e/l=0.3. Three actuators distributed uniformly along the axis of the beam are bonded on the top surface of the beam, and six sensors are attached on the bottom surface of the beam. Finite element analysis based on the theory described in the previous section is employed to solve the problem with 20 linear finite elements.

5.1 Natural Frequencies

The first ten natural frequencies of the beam are calculated and compared to those of its undelaminated counterpart in Table 1. There are not remarkable differences in frequencies between the two models for the first five modes. The 6th natural frequency of the delaminated beam (1140.110Hz) is identified as a delamination mode which is a non classical mode shape(Fig. 3). This special mode can lead to response differences from an undelaminated beam. As noted by Hanagud et al. (1992), however, it may be difficult to detect the size and the location of the delamination from the time response data. Furthermore, it is not easy to assess the delamination by this high frequency excitation. Therefore, the actuator forces should be optimized such that the delaminated beam can be excited to maximize the response difference from the undelaminated beam even for low excitation frequencies.

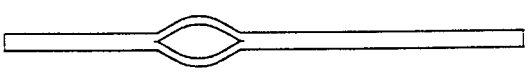

Fig. 3 Delamination Mode at 1140.1 Hz

Table 1 Natural frequencies of delaminate and undelaminated beams

	Delaminated(Hz)	Undelaminated(Hz)
1	35.91	36.14
2	144.55	145.75
3	293.35	332.57
4	541.31	603.02
5	922.77	966.64
6	1140.10	1436.67
7	1207.85	2030.88
8	1751.60	2772.62
9	2390.73	2806.10
10	2800.28	3602.31

5.2 Weighting Parameter

To show the effect of the weighting parameter λ, the response ratio E_3 was maximized for increasing values of λ by the eigenvalue problem (15). For each case, the corresponding values of E_1 and E_2 are given in Table 2. In this example, the excitation frequency (ω) was half of the first natural frequency of the undelaminated beam (ω_1).

For $\lambda=0$ the value of E_2 falls between the square of the first (0.051×10^{-6}) and the second (0.825×10^{-6}) natural frequencies, which are not very high frequencies. Consequently, the displacement fields for $\lambda=0$ are not associated with very high frequency vibration modes, and this λ value gives a reasonable approximation for strain energy anti-optimization. As λ increases, E_1 and E_2 approach 1 and the squar e of the first natural frequency, respectively. Substantial changes in E_1 and the eigenvector f do not occur until λ reaches 10^5. For all cases, the combined ratio E_3 was always found to be greater than 1.

Table 2 E1 and E2 ($\times10^{-6}$) as a function of λ for excitation frequency equal to 0.5 ω_1

λ	E_1	E_2	f_1	f_2	f_3
0	1.364	0.653	-0.879	1	-0.481
10^3	2.364	0.589	-0.877	1	-0.478
10^4	1.300	0.144	-0.808	1	-0.418
10^5	1.023	0.051	-0.229	1	0.350

5.3 Effects of Errors

In many practical situations, measurement noise and modelling errors may be significant. To simulate such noise and errors, matrix $\hat{K}$ in Eq. (21) calculated from the strain energy anti-optimization are perturbed as follows:

$$\hat{K}_{ij} = [1+N(2R-1)]\hat{K}_{ij}, \tag{29}$$

where N is a noise amplitude and R is a random number uniformly distributed between zero and one.

In general, beams are not perfect geometrically, and have variations in material properties and geometry. Such imperfections are simulated through random thickness of each finite element is allowed to vary within 5% combined with the variation of $\hat{K}$matrix. The relative errors of two extreme eigenvalues defined as

$$\Delta E = \frac{|E_{\text{perturbed}} - E_{\text{exact}}|}{E_{\text{exact}}} \tag{30}$$

and the angles between exact and perturbed eigenvectors are presented in Table 3. For $\omega/\omega_1 = 05$, the results are shown to be sensitive to the variation of $\hat{K}$ with more than 1% noise of measurement error producing unacceptable errors. At excitation frequency close to the resonance, the results are too sensitive to be meaningful. This is because of the unstable nature of $\hat{K}$ matrix near the resonance. Thus, this excitation frequency is not appropriate for identification. For higher excitation frequencies, the results are much less sensitive to the measurement noise. For $\omega/\omega_1 = 2$ the angle between exact and perturbed eigenvector dif-

fer only 3° even for 5% measurement noise. This excitation frequency is found to be the best among the frequencies considered. For all the cases, the effect of thickmess variation seems to be neglible compared to the measurement noise.

Table 3 Effect of the number of strain sensors for $\omega/\omega_1 = 5$

Number of Strain sensors	Actuators			
	E_3	f_1	f_2	f_3
3	3.816	0.71	1	0.689
4	2.738	1	-0.207	0.899
6	1.549	0.752	1	0.593
10	1.870	1	0.512	0.908
20	1.982	1	0.616	0.931
Strain Energy Solution	E3=2.055	1	0.617	0.937

4. Delamination Detection

The actuator magnitude ratios which maximize the strain energy ratio are obtained for three different excitation frequencies. The derivative of the residual force is calculated for every possible simulated delamination with size 10% of beam length from node 1 to node 21, and is plotted through the axial location of the beam in Fig. 4 for with and without measurement noise in $\hat{K}$. For each finite element node, these three values are multiplied to help finding peaks and it is presented in Fig. 5. There are two peaks in Fig. 5, and delaminated region is found to be either of these two locations of the beam.

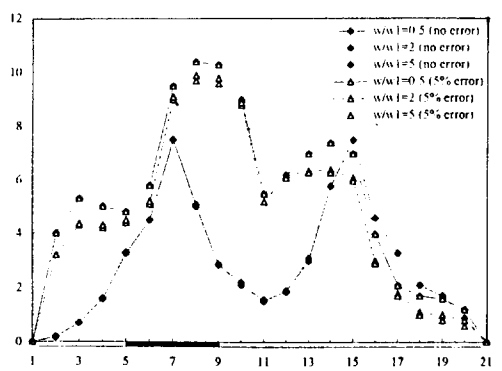

Fig. 4 The derivative of residual force for a delamination at d/ l=0.3

It should be noted that the location corresponding to the higher peak is not necessarily the location of delamination. Thus, both can didate locations of delamination are further in vestigated by using the method described in the section 4. The location of C_1 and C_2 can be estimated based on Fig. 5 as

C_1 : delaminated at node 7
C_2 : delaminated at node 15 (31)

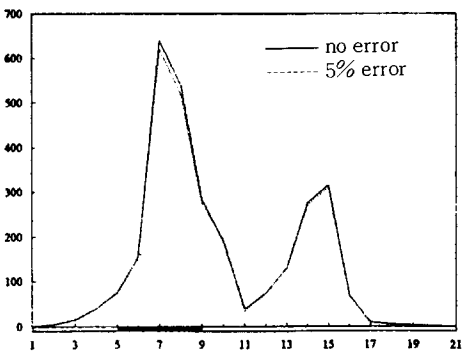

Fig. 5 The derivative of residual force for a delamination at e/ l=0.3(multiplied)

Table 4 Estimation of the location of a delamination

Candidate	$\omega/\omega 1$	E_3	Actuators			
			f_1	f_2	f_3	
C1	0.5	1.051	-0.894	1	-0.474	0.605
(node 7)	2	1.053	-0.948	1	-0.605	0.908
	5	1.146	1	0.736	-0.927	4.128
C2	0.5	1.051	-0.474	1	-0.894	23.517
(node 15)	2	1.053	-0.605	1	-0.948	18.487
	5	1.146	0.927	0.736	1	5.48

The eigenvectors for the two candidates are calculated by using anti-optimization, and the

angles for both candidated are presented in Table 4 for fjour different excitation frequencies. For all the external frequencies considered, the angles associated with C_1 are smaller than thouse associated with C_2.

In fact, either C_1 or C_2 does not exactly correspond to the actual location and size of delamination. For low excitation frequencies, the error angle θ between the actual location and the C_1 is small. As frequency increases, the angle becomes larger for C_1, but the error angle for C_2 decreases. This is because C_2 has a mirror image to the actual delamination location, and it becomes indistinguishable for larger wave numbers. That is, for more accurate estimation of delamination location, higher frequencies may be necessary, where as low frequencies are preferable for selecting a candidate which is closer to actual delamination location. Consequently, C_1 is the estimated location of delamination.

Once after the location of a delamination is estimated, the next step is to determine the size of the delamination. The delamination size can be detected by comparing the measured eigenvalues with eigenvalues of candidates. The candiates are produced by increasing the size of the delamination which is neighboring nodes of C_1. As shown in Table 5, it can be concluded that any of the entries except the one with only node 8 corrupted can be a solution (observe ΔE).

Table 5 Estimation of the size of a delamination

Corrupted nodes	E_3	Actuators			ΔE_3
		f_1	f_2	f_3	
7	1.051	-0.894	1	-0.474	0.235
6,7	1.112	-0.867	1	-0.485	0.185
7,8	1.208	-0.897	1	-0.473	0.114
5,6,7	1.179	-0.92	1	-0.461	0.136
6,7,8	1.364	-0.879	1	-0.481	0
7,8,9	1.524	-0.9	1	-0.474	0.117

6. Concluding Remarks

In this paper, a technique wihich can detect a delamination in laminated beams is presented. Using anti-optimization, the optimal excitation parameter is obtained which extremize the difference between nominal and delaminated beams. And then, the location and the size of a delamination is estimated by using the excitation parameter obtained from anti-optimization in con juction with system identification. In order to validate the reliability of the theoretical model, geometric and measurement noise situations are numerically. simulated. It is found that the present anti-optimization based system identification technique detects the size and the location of delamination succesfully.

REFERENCES

1. Hanagud, S., Babu, G. L. N., Roglin, R. L. and Savanur, S. G., 1992 Active Control of Delaminations in Composite Structures, Presented at the 33th AIAA/ASME/ASCE/ASC SDM Conference, Dallas, Tx.
2. Teboub, Y. an Hajela, P., 1992 A Neural Network Based Damage Analysis of Smart Composite Beams, Presented at the 4th AIAA/USAF/NASA/OAISymposium on Multidisplinary Analysis and Optimization, Cleveland, OH.
3. Kim, K., Segall, A. and Springer, G., 1993, The Use of Strain Measurements for Detecting Delaminations in Composite Laminates, Composite Structures, 23 : 75-84.
4. Lee, J., Gürdal, Z. and Griffin, O. H., 1993, Layer Wise Approach for the Bifurcation Problem in Laminated Composites with Delaminations, AIAA Journal, 31 : 331−338.
5. Haftka, R. T. and Kao, P.J., 1990, The Use of Optimization for Sharpening Differences be-

tween Models, Paper presented at the ASME Winter Annual Meeting, Dallas, TX.
6. Gangadharan, S. N., Nikolaidis, E. and Haftka, R. T., 1991, Probabilistic System Identification of Two Flexible Joint Models, Aiaa Journal, 29 : 1319−1326.
7. Chen, J. C. and Garba, J. A., 1989, On-Orbit Damage Assessment for Large Space Structures, AIAA Journal, 26 : 1119−1126

(접수일자 : 1996. 5. 18)